Published in final edited form as:
Mol Imaging. 2008 ; 7(4): 187–197.

Radiosynthesis and Evaluation of 5-[^{125}I]Iodoindol-3-yl-β-D-galactopyranoside ([^{125}I]IBDG) as a β-Galactosidase Imaging Radioligand

Marcian E. Van Dort[*,1,3], **Kuei C. Lee**[1,3], **Christin A. Hamilton**[2,3], **Alnawaz Rehemtulla**[2,3], and **Brian D. Ross**[1,3]

[1]Department of Radiology, University of Michigan Medical School, Ann Arbor, MI 48109-2200.

[2]Department of Radiation Oncology, University of Michigan Medical School, Ann Arbor, MI 48109-2200.

[3]Center for Molecular Imaging, University of Michigan Medical School, Ann Arbor, MI 48109-2200.

Abstract

The synthesis and investigation of 5-[^{125}I]Iodoindol-3-yl-β-D-galactopyranoside ([^{125}I]IBDG) as a radioligand for single photon emission computed tomography (SPECT) imaging of β-galactosidase expression is described. No-carrier-added [^{125}I]IBDG was synthesized by a radioiododestannylation approach in >75% overall radiochemical yield and >99% radiochemical purity. [^{125}I]IBDG was evaluated as a substrate using β-galactosidase-expressing (*D54L*) and non-expressing (*D54*) human glioma cell lines. A 24 h incubation of this substrate with cultured cells revealed a 6.5-fold greater intracellular trapping of radioactivity in *D54L* cells compared to *D54* cells. Systemic delivery of [^{125}I]IBDG in nude mice bearing *D54L* tumors failed to show significant trapping of radioactivity within these tumors by SPECT imaging. In contrast, intratumoral injection of the substrate resulted in efficient trapping of radioactivity in *D54L* tumors but not *D54* tumors resulting in clear SPECT visualization of the former tumor. Based on dynamic SPECT imaging and blood metabolite analysis, we conclude that although [^{125}I]IBDG is an efficient *in vivo* substrate for β-galactosidase, its rapid renal clearance hampers its intratumoral availability upon systemic administration.

Keywords

gene expression imaging; β-galactosidase; iodine-125; SPECT; PET

INTRODUCTION

Expression of a reporter gene under the control of specific enhancer/promoter sequences is a widely used strategy for monitoring of gene regulation in biological systems. Reporters used for gene expression monitoring include β-galactosidase, chloramphenicol acetyltransferase, β-glucoronidase, firefly luciferase and green fluorescent protein.1 Among these, the bacterial enzyme *Escherichia coli* β-galactosidase (β-gal), expressed by the *lacZ* gene is the reporter most commonly used due to its high stability and turnover rate, ease of conjugation and detection and lack of endogenous expression in eukaryotic cells.2 *LacZ* expression and

Corresponding Author Address: Center for Molecular Imaging, Department of Radiology, University of Michigan Medical School, A668 BSRB, 109 Zina Pitcher Place, Ann Arbor, MI 48109-2200, Phone: 734-615-2280; Fax: 734-763-5447, E-mail: mvandort@umich.edu.

consequently gene transfection levels can thus be conveniently monitored by utilizing suitable β-gal substrates that exhibit a physical change (e.g. colorimetry, fluorescence) upon enzymatic hydrolysis.[3, 4]

The ability to noninvasively monitor the location, magnitude and persistence of heterologous gene expression *in vivo* is critical for many studies in medical research.[5–7] Consequently, this has led to intense interest in the development of β-gal substrates as imaging probes for *in vivo* imaging of gene expression. Reports describing a variety of such substrates for far-red fluorescence,[2, 8–10] bioluminescence[11] and magnetic resonance[12] imaging have appeared in the recent literature. In contrast, there have been very few reports concerning the development of radioligands for either single photon emission computed tomography (SPECT) or positron emission tomography (PET) imaging of β-gal expression. A radioiodinated β-gal inhibitor for SPECT imaging of β-gal expression has been described by Choi and coworkers, however, *in vivo* studies with this radioligand were not encouraging which was attributed, in part, to its low cell membrane permeability.[13, 14] From a clinical standpoint, SPECT and PET imaging techniques offer several unique advantages compared to the aforementioned imaging modalities including high sensitivity, improved safety due to administration of subpharmacological doses, ability to visualize gene expression tomographically and ease of external imaging of deep tissues. Furthermore, PET and SPECT imaging techniques of gene expression will likely have greater clinical utility than fluorescence or bioluminescence-based methods due to the wider availability of nuclear medicine imaging facilities. Our efforts to develop a radioiodinated substrate for SPECT/PET imaging of β-gal-expressing tumors focused on the known chromogenic β-gal substrate: 5-Iodoindol-3-yl-β-D-galactopyranoside (Purple-β-D-Gal; IBDG; Figure 1). Intracellular enzymatic hydrolysis of β-gal substrates such as IBDG generates free indoxyl molecules which undergo *in situ* oxidation and subsequent dimerization to produce chromogenic, water-insoluble, indigo precipitates (Figure 2).[15] We hypothesized that use of a radioiodinated IBDG derivative could by a similar process lead to selective retention of the radiolabel in β-gal-expressing cells thus permitting *in vivo* imaging of β-gal expression by SPECT or PET techniques. As a step towards this goal, the radiosynthesis and preliminary biological evaluation of [^{125}I]IBDG was undertaken and these studies are herein reported.

MATERIALS AND METHODS

Chemicals and Radiochemicals

N-Acetyl-5-bromoindol-3-ol was purchased from Apollo Scientific Ltd., Cheshire, UK and IBDG was purchased from Biotium, Inc., Hayward, CA. All other chemical reagents were obtained from Aldrich Chemical Co., Milwaukee, WI. Sodium [^{125}I]iodide was obtained from MDS Nordion Inc. (Ottawa, Canada) as a no-carrier-added solution in aqueous 0.01 N NaOH (pH 10 – 12).

Instrumentation and Analyses

Melting points were determined with a Thomas-Hoover melting point apparatus and are uncorrected. Thin-layer chromatography (TLC) was performed using Analtech silica gel GF Uniplates (250 micron). TLC plates were visualized after development using either ultraviolet (UV) light or phosphomolybdic acid reagent with subsequent heating. ^{1}H NMR spectra were recorded on a Varian INOVA instrument operating at 400 MHz with either $CDCl_3$ or DMSO-d_6 as solvent and tetramethylsilane (TMS) as internal standard. Chemical shifts (δ) and coupling constants (*J*) are reported in parts per million (ppm) and Hertz (Hz), respectively. Compound elemental analysis data were obtained at the Department of Chemistry, University of Michigan. High resolution mass spectral analyses were performed at the Department of Chemistry, University of Michigan, using either a VG-70-250-S mass

spectrometer for electron impact (EI) and chemical ionization (DCI) modes or a Waters Autospec Ultima instrument with an electrospray interface for electrospray ionization (ESI) mode. HPLC was performed using a Waters Breeze HPLC System (Waters Corporation, Milford, MA) equipped with a Waters 2487 Dual Wavelength Absorbance Detector. Radioactivity was monitored with a Bioscan Flow Count FC-3300 NaI/PMT Radiodetector (Bioscan, Inc., Washington, DC) equipped with a 1.5" × 1.5" NaI(Tl) crystal. Radio-HPLC analysis and purification were conducted with a Supelcosil LC-C18 analytical column (4.6 × 250 mm, 5 μ particle, Supelco, Bellefonte, PA) using HPLC grade water (A) and CH_3CN (B) solvent mixtures with either of the following methods: Method I (solvent gradient elution from 55% B to 95% B over 20 min; UV detection at 254 nm); Method II (solvent gradient elution from 10% B to 95% B over 20 min; UV detection at 280 nm). All chromatographic procedures were conducted at ambient temperature using a flow rate of 1 mL/min.

Radioactivity measurements were obtained with a Capintec CRC-15W Radioisotope Dose Calibrator (Ramsey, NJ) and specific activity estimates were determined from a standard curve relating mass to UV absorbance peak area.

Synthetic Chemistry

1-Acetyl-5-bromoindol-3-yl-*tetra*-*O*-acetyl-β-D-galactopyranoside (3)—The title compound was synthesized from 2,3,4,6-*tetra*-*O*-acetyl-β-D-galactopyranosyl bromide (**1**) and *N*-acetyl-5-bromoindol-3-ol (**2**) according to the method of Horwitz *et. al.*.16 Flash chromatography of the crude product on silica gel (40% EtOAc/hexanes) followed by recrystallization from ethanol provided **3** in 43% yield: mp 175 – 176 °C. ^{1}H NMR ($CDCl_3$): δ 8.26 (br s, 1H), 7.62 (d, 1H, *J* = 1.7 Hz), 7.47 (dd, 1H, *J* = 9.0, 1.9 Hz), 7.16 (br s, 1H), 5.56 – 5.48 (m, 2H), 5.12 (dd, 1H, *J* = 10.5, 3.5 Hz), 4.97 (d, 1H, *J* = 8.0 Hz), 4.23 (m, 2H), 4.06 (t, 1H, *J* = 6.9 Hz), 2.60 (s, 3H), 2.21 (s, 3H), 2.15 (s, 3H), 2.07 (s, 3H), 2.04 (s, 3H). HRMS: Calcd for $C_{24}H_{26}BrO_{11}NNa$: 606.0587. Found: 606.0567. Anal. Calcd for $C_{24}H_{26}NBrO_{11}$: C, 49.33; H, 4.48; N, 2.40. Found: C, 49.02; H, 4.41; N, 2.30.

1-Acetyl-5-(tributylstannyl)indol-3-yl-*tetra*-*O*-acetyl-β-D-galactopyranoside (4)—A solution of the bromoindole analog **3** (0.438 g, 0.75 mmol) and bistributyltin (1.74 g, 3.0 mmol) in anhydrous toluene (12 mL) was degassed with a nitrogen stream for 10 min and treated with tetrakis(triphenylphosphine)Pd(0) (0.087 g, 0.075 mmol) in one portion.17 The mixture was refluxed with stirring under a nitrogen atmosphere for 18 h, at which point, TLC analysis showed completion of reaction. The warm mixture was filtered through a pad of Celite and concentrated *in vacuo* to give a brown gum. Flash chromatography of the residue on silica gel (40% EtOAc/hexanes) provided 0.21 g (35%) of pure material as an off-white amorphous solid. ^{1}H NMR ($CDCl_3$): δ 8.30 (br s, 1H), 7.59 (s, 1H), 7.46 (d, 1H, *J* = 8.2 Hz), 7.15 (br s, 1H), 5.60 – 5.56 (m, 1H), 5.49 (m, 1H), 5.13 (dd, 1H, *J* = 10.5, 3.3 Hz), 5.00 (d, 1H, *J* = 8.0 Hz), 4.24 (d, 2H, *J* = 6.4 Hz), 4.08 (t, 1H, *J* = 6.3 Hz), 2.60 (s, 3H), 2.20 (s, 3H), 2.11 (s, 3H), 2.08 (s, 3H), 2.03 (s, 3H), 1.57 – 1.52 (m, 6H), 1.38 – 1.29 (m, 6H), 1.11 – 1.07 (m, 6H), 0.89 (t, 9H, *J* = 7.33 Hz). HRMS: Calcd for $C_{36}H_{53}O_{11}NSnNa$: 818.2538. Found: 818.2545.

1-Acetyl-5-iodoindol-3-yl-*tetra*-*O*-acetyl-β-D-galactopyranoside (5)—A stirred solution of the tributylstannyl analog **4** (0.155 g, 0.20 mmol) in anhydrous $CHCl_3$ (15 mL) was treated dropwise with a 0.1 M solution of iodine in $CHCl_3$ until a slight violet color persisted. The solution was stirred a further 3 h at room temperature and quenched with a solution of KF in CH_3OH (1 M, 0.5 mL) followed by aqueous 5% $NaHSO_3$ solution (1.5 mL). The mixture was treated with saturated brine (5 mL) and the organic layer separated and dried (Na_2SO_4). Flash chromatography of the residue on silica gel (40% EtOAc/

hexanes) gave 0.10 g (79%) of the title compound **5** as a white solid following recrystallization from ethanol : mp 189 – 191 °C (dec) ^{1}H NMR ($CDCl_3$): δ 8.14 (br s, 1H), 7.82 (d, 1H, *J* = 1.6 Hz), 7.65 (dd, 1H, *J* = 8.7, 1.7 Hz), 7.13 (br s, 1H), 5.56 – 5.48 (m, 2H), 5.12 (dd, 1H, *J* = 10.5, 3.5 Hz), 4.96 (d, 1H, *J* = 7.8 Hz), 4.23 (m, 2H), 4.06 (t, 1H, *J* = 5.9 Hz), 2.59 (s, 3H), 2.21 (s, 3H), 2.16 (s, 3H), 2.07 (s, 3H), 2.04 (s, 3H). HRMS: Calcd for $C_{24}H_{26}IO_{11}NNa$: 654.0448; Found: 654.0453. Anal. Calcd for $C_{24}H_{26}NIO_{11}$: C, 45.66; H, 4.15; N, 2.22. Found: C, 45.37; H, 4.24; N, 2.33.

5-Iodoindol-3-yl-β-D-galactopyranoside (IBDG)—Sodium methoxide (0.02 mL, 0.01 mmol, 0.5 M in methanol) was added to a stirred solution of the pentaacetate analog **5** (0.025 g, 0.040 mmol) in anhydrous methanol (2 mL) at 5 °C. The clear solution was stirred for an additional 1 h and allowed to stand at 5 °C overnight. The reaction was neutralized with 1 drop of 50% aqueous acetic acid and the mixture concentrated to dryness *in vacuo* at room temperature. Flash chromatography of the residue on silica gel (15% methanol/ dichloromethane) followed by recrystallization from water gave 13 mg (77%) of the title compound as a white solid. mp 180 – 182 °C (*dec*) ^{1}H NMR (DMSO-d_6 + 1 drop D_2O): δ 7.94 (d, 1H, *J* = 1.4 Hz), 7.29 (dd, 1H, *J* = 8.6, 1.6 Hz), 7.15 (d, 1H, *J* = 8.6 Hz), 7.06 (s, 1H), 4.46 (d, 1H, *J* = 7.6 Hz), 3.65 (d, 1H, *J* = 3.1 Hz), 3.58 – 3.49 (m, 3H), 3.43 (t, 1H, *J* = 6.2 Hz), 3.35 (dd, 1H, *J* = 9.6, 3.3 Hz). HRMS: Calcd for $C_{14}H_{16}IO_6NNa$: 443.9920; Found: 443.9918. Anal. Calcd for $C_{14}H_{16}NIO_6$: C, 39.92; H, 3.83; N, 3.33. Found: C, 40.04; H, 3.90; N, 3.27.

Radiosynthetic Chemistry

1-Acetyl-5-[^{125}I]iodoindol-3-yl-*tetra-O*-acetyl-β-D-galactopyranoside ([^{125}I]5)— A glass vial containing a solution of **4** (30 μg, 38 nmol) in absolute ethanol (30 μL) was treated with a solution of 50 μL of freshly prepared 0.1 N HCl in ethanol. The vial was sealed and crimped, a solution of 6.13 mCi of $Na^{125}I$ in aqueous 0.01 N NaOH (6.0 μL) was added by syringe to the vial and the reaction was initiated by addition of 50 μL of freshly prepared aqueous H_2O_2 (3% wt./vol.). The vial was shaken periodically for 10 min and the reaction was quenched by addition of 100 μL of aqueous sodium metabisulfite (12 mg/mL). HPLC analysis of the crude product mixture (Method I) showed 95% radiochemical purity for **[^{125}I]5** (t_R = 10.1 min). The crude product was purified by preparative HPLC (Method I) to afford 5.05 mCi (82%) of **[^{125}I]5** (>99% chemical and radiochemical purity) which was concentrated to dryness *in vacuo* and used directly in the next step.

5-[^{125}I]Iodoindol-3-yl-β-D-galactopyranoside ([^{125}I]IBDG)—A solution of no-carrier-added **[^{125}I]5** (5 mCi) in anhydrous methanol (0.5 mL) was cooled to 5 °C (ice-bath) under a nitrogen atmosphere. A 0.5 M solution of sodium methoxide in methanol (15 μL) was then added by syringe and the reaction mixture was maintained at 5 °C for 60 min. The mixture was quenched with 50% aqueous acetic acid (10 μL), concentrated *in vacuo* and purified by preparative HPLC (Method II; t_R of IBDG = 8.5 min). The HPLC fraction containing the product was diluted with water (10 mL) and eluted through a preconditioned C-18 Sep-Pak cartridge. The cartridge was eluted with CH_3CN (2 mL) to afford **[^{125}I]IBDG** which was concentrated under reduced pressure and formulated in PBS:EtOH [95:5] for animal studies. The chemical identity of **[^{125}I]IBDG** was confirmed using analytical HPLC (Method II) by co-injection with the nonradioactive IBDG standard.

Cell Culture and Transfections

D54 (human glioma) cells were grown in RPMI 1640 medium supplemented with 10% fetal bovine serum, 100 units/ml penicillin, 100 μg/ml streptomycin sulfate, 1 mM sodium pyruvate, 10 mM HEPES, 292 ng/ml L-glutamine (all from Invitrogen, Carlsbad CA) and maintained in a humidified incubator at 37 °C and 5% CO_2. Cells were transfected using 4

μg of pEFLacZ and 16 μL of Fugene according to the manufacturer's protocol. Stable clones were selected using 200 ng/ml G418 (Invitrogen) and characterized for expression of the reporter. Specific clones were identified and selected for further study based on expression levels of the recombinant protein.

Detection of β-gal Activity *In Vitro* with [^{125}I]IBDG

In vitro studies to detect β-gal activity using [^{125}I]IBDG were conducted using control D54 human glioma cells (*D54*) and their β-gal expressing counterpart (*D54L*). Cells were seeded in 6-well dishes and incubated for up to 48 h at 37 °C with no-carrier-added [^{125}I]IBDG (0.1 μCi per well) together with various concentrations of cold IBDG substrate (0 mM, 0.5 mM and 1.0 mM). Cells were collected by scraping after 24 h and 48 h of incubation and pelleted by centrifugation at 1800 rpm for 10 min. After removal of the supernatant, the pellet was rinsed with PBS and re-pelleted. Finally, the pellet was re-suspended in PBS and assayed for radioactivity using a Gamma Counter.

Animal Models

Athymic, CD1 nude mice (nu/nu; 25 – 30 g; 5 – 6 weeks old; N = 6; Charles River Laboratories, IN) were used for the tumor imaging studies. For systemic (i.v., i.p.) injection studies, mice under isoflurane anesthesia were initially injected subcutaneously in each flank with equivalent amounts (2×10^6 cells) of either *D54L* (right flank) or *D54* tumor cells (left flank). Tumors were allowed to grow to approximately 5 – 7 mm in size prior to conducting imaging studies. Animals under isoflurane anesthesia were injected (i.v. or i.p.) with [^{125}I]IBDG (500 μCi in 100 μL of PBS:EtOH [95:5]; specific activity = 5 mCi/mg) and a series of image acquisitions (10 – 60 min) were collected at 5 min, 1 h, 2 h, 4 h, 7 h, 12 h and 24 h post-injection.

For the intratumoral injection studies, mice under isoflurane anesthesia were initially injected subcutaneously in each flank with equivalent amounts (10^7 cells in 200 μL of PBS) of either *D54L* (right flank) or *D54* tumor cells (left flank). Each tumor implantation site was then directly injected with equivalent doses of [^{125}I]IBDG (500 μCi in 100 μL of PBS:EtOH [95:5]; specific activity = 5 mCi/mg; approximately 0.5 mM concentration in tumor) and a series of image acquisitions (10 – 60 min) were collected at 5 min, 1 h, 2 h, 4 h, 7 h, 12 h and 24 h post-injection.

All animal studies were conducted in accordance with the rules of the University Committee on Use and Care of Laboratory Animals (UCUCA) at the University of Michigan.

SPECT/CT Mouse Imaging Studies

SPECT/CT imaging studies were conducted on a GMI Tri-Modality CT/PET/SPECT small animal scanner (Gamma-Medica Ideas, Inc., Northridge, CA). SPECT images were acquired using a dual-head, high-resolution, low-energy parallel-hole collimator. CT imaging of animals was performed for anatomical co-registration and CT fusion of SPECT images were performed using AMIRA (version 3.1) software.

Analysis of Mouse Blood Metabolites of [^{125}I]IBDG

Tumor-bearing CD1 mice (N = 3) under isoflurane anesthesia were each injected intravenously with approximately 600 μCi of [^{125}I]IBDG in 0.2 mL 0f PBS:EtOH [95:5] and sacrificed 5 min post-injection. Blood samples (approximately 0.6 – 0.8 mL) were collected by cardiac puncture and homogenized with equal volumes of acetonitrile. The mixture was centrifuged at 15,000 g for 20 min, the supernatant was transferred to a fresh centrifuge tube (95% extraction efficiency) and the centrifugation repeated. The clear

supernatant was concentrated using a nitrogen stream and analyzed by radio-TLC (silica; CH_2Cl_2:CH_3OH [4:1]) and HPLC analysis (Method II).

Determination of Partition Coefficient of IBDG

The partition coefficient (P) of IBDG was determined by modification of a "shake-flask technique" as described by Rothwell *et al.*18 n-Octanol and potassium phosphate buffer (20 mM, pH 7.4) were pre-saturated with each other for 24 h prior to use. Solutions of IBDG (1 – 2 mM) in 2 mL of potassium phosphate buffer were combined with an equal volume of n-octanol in a centrifuge tube and vortexed for 1 min. The mixture was then centrifuged at 5000 rpm for 5 min and the layers separated. The concentration of IBDG in each phase was determined from the corresponding UV peak areas following HPLC analysis (Method II; UV analysis at 215 nm). Samples of n-octanol were diluted with 4 volumes of acetonitrile prior to HPLC injection. Partition experiments were conducted in triplicate and HPLC analysis of each phase was conducted in duplicate. The partition coefficient is defined as the ratio of the concentration of substance in n-octanol to that in buffer and lipophilicity (log P) is reported as the logarithm of the partition coefficient. IBDG displayed a log P of 0.8 in these experiments.

RESULTS

Chemistry

Our synthetic strategy for preparation of radioiodinated IBDG focused on the use of the tributylstannyl analog **4** as a precursor for radiolabeling (Scheme 2). The synthesis of **4** and cold IBDG are shown in Scheme 1. In this approach, we utilized *N*-acetyl-5-bromoindol-3-ol (**2**) instead of the corresponding iodo analog as the aglycone in the initial reaction step due to its lower cost and commercial availability. Initial attempts at synthesizing the acetyl-protected galactoside derivative **3** by reaction of **2** with galactopyranosyl bromide (**1**) under phase-transfer catalysis conditions19› 20 resulted in complex product mixtures and poor isolated yields. Subsequently, compound **3** was prepared in moderate yield (43%) according to the method of Horvitz *et al.* by a base-catalyzed reaction of **2** with galactopyranosyl bromide (**1**).16 Replacement of the bromine atom in intermediate **3** with the tributylstannyl group was achieved via a palladium-mediated coupling reaction using bistributyltin and tetrakis(triphenylphosphine)palladium(0) as catalyst to afford **4** in 35% yield. A portion of this material was converted to the corresponding acetyl protected IBDG derivative (**5**) by an iododestannylation reaction with iodine in chloroform. Deacetylation of the latter intermediate using Zemplen conditions (NaOMe/MeOH) followed by chromatographic purification provided cold IBDG in 77% yield. All of the synthesized compounds displayed H-1 NMR and mass spectra consistent with the assigned structures. The *trans* configuration of the 1,2 glycoside bond (β-anomer) in the galactoside derivatives was confirmed by the presence of a characteristic doublet for the anomeric proton signal at δ 4.46 – 5.0 ($J_{1,2}$ 7.6 – 8.0 Hz) in their NMR spectra.

Radiosynthetic Chemistry

The synthesis of no-carrier-added [^{125}I]IBDG was accomplished using a radioiododestannylation approach (Scheme 2).17 Accordingly, the tributylstannyl analog **4** was treated with Na^{125}I and aqueous H_2O_2 as oxidizing agent to afford crude **[^{125}I]5** in 95% radiochemical purity. Further purification of this material by preparative reversed-phase HPLC provided **[^{125}I]5** in 82% overall radiochemical yield and >99% radiochemical purity. Subsequent deacetylation of **[^{125}I]5** was conducted using sodium methoxide in methanol at 5 °C to afford [^{125}I]IBDG in 92% radiochemical yield and >99% radiochemical and chemical purity after HPLC purification. The average specific activity of [^{125}I]IBDG was 1685 ± 153 Ci/mmol (N = 5). The radioligand which was formulated in PBS:EtOH [95:5]

was stable for at least 1 week when stored at 5 °C (<2% radiolytic decomposition by radio-HPLC analysis).

In Vitro Cell Uptake Studies

The ability of [^{125}I]IBDG to undergo cellular uptake and retention was investigated in β-gal-expressing D54 cells (*D54L*) in comparison to control cells (*D54*).14, 21 Initial validation studies with cold IBDG using a colorimetric assay showed that optimum conversion of this substrate in *D54L* cells occurs at a 24 – 48 h incubation time with a 0.5 – 1.0 mM substrate concentration (Figure 3). Subsequent studies conducted with [^{125}I]IBDG demonstrated a 6.5- to 7-fold increase in cellular radioactivity in *D54L* cells compared to *D54* controls following a 24 h to 48 h incubation period at 0.5 mM substrate concentrations (Figure 4; 48 h data not shown). Radioactivity uptake ratios were somewhat lower (4.5- to 5.1-fold) at these same time intervals at 1.0 mM substrate concentrations (data not shown). No significant difference in radioactivity uptake was observed between the two cell types for either time interval at no-carrier-added levels of [^{125}I]IBDG (0 mM).

SPECT Imaging Studies

A) Systemic [^{125}I]IBDG administration—Mouse SPECT/CT imaging studies were conducted over a 24 h period after intravenous administration of [^{125}I]IBDG. Analysis of the image data showed high initial uptake of radioactivity in kidney within 5 min after injection followed by its excretion into urinary bladder over a 1 – 2 h period. Radioactivity uptake in most major organs were at or near background levels throughout the imaging study. Neither the *D54L* nor *D54* tumor was visualized in the SPECT images during the entire imaging time frame due to insufficient tumor uptake of radioactivity. A similar pharmacokinetic behavior was seen in the SPECT images following i.p. administration of the radioligand.

B) Intratumoral [^{125}I]IBDG administration—Serial SPECT/CT imaging studies were also conducted as described above following the intratumoral injection of [^{125}I]IBDG. The mouse SPECT image (A) and temporal tumor distribution profile (B) data at 5 min, 2 h and 4 h post-injection are shown in Figure 5. As seen from this data, a sharp decline of radioactivity for the *D54* tumor as compared to the *D54L* tumor is clearly apparent at the 2 h imaging interval. Clearance of radioactivity from the *D54* site was essentially complete by 7 h post-injection, while radioactivity levels in the *D54L* tumor were similar to its 4 h values (data not shown). This differential resulted in clear visualization of the β-gal expressing *D54L* tumor within the 2 h, 4 h and 7 h images. Radioactivity clearance occurred mainly via the renal pathway as evidenced by high urinary bladder radioactivity and the absence of radioactivity in liver.

Mouse Blood Metabolite Analysis

Radio-HPLC analysis of mouse blood radioactivity at 5 min post-injection showed that approximately 39% of the total radioactivity was associated with intact [^{125}I]IBDG. The remaining radioactivity consisted primarily of two polar metabolites eluting at t_R = 2.8 min (16%) and t_R = 3.3 min (53%), respectively. Neither of the polar metabolites were ^{125}I as confirmed by HPLC analysis with co-injected sodium iodide. A similar metabolite profile was seen by radio-TLC analysis.

DISCUSSION

β-galactosidase is a stable, quantitative and sensitive reporter extensively used for gene expression studies. For example, studies involving promoter function in transgenic animals as well as gene delivery studies in animal models have utilized the β-gal gene.22–24 However, these studies invariably involve sacrifice of the animal and subsequent extraction

of the desired tissues for detection of expression. Consequently, such studies only provide a snapshot image of β-gal expression. The use of noninvasive tomographic imaging techniques such as PET or SPECT can provide real-time, quantitative information of biochemical or molecular processes repetitively in the same subject. Such methods when applied to gene expression imaging could therefore provide the means to follow β-gal expression longitudinally in living subjects which would be of great value both for preclinical studies and future clinical gene therapy trials.5

A wide variety of galactoside analogs that are β-gal enzyme substrates are routinely available for spectroscopic analysis of β-galactosidase activity. Enzymatic hydrolysis of these substrates leads to the formation of an intensely-colored, water-insoluble, reaction product which is selectively localized to the site of reporter gene expression and can be conveniently monitored by colorimetry. The goal of the present study was to synthesize and evaluate a suitably radioiodinated β-gal substrate that would exploit this selective trapping mechanism for *in vivo* imaging of β-gal expression using SPECT. For this purpose, we focused on the chromogenic β-gal substrate: 5-iodoindol-3-yl-β-D-galactopyranoside (IBDG) as a candidate for radioiodination and biological evaluation. For these initial studies, we radioiodinated IBDG with ^{125}I instead of the standard SPECT radioisotope ^{123}I due to its lower cost, longer half-life and its imaging capability with dedicated small animal SPECT scanners. Radiosynthesis of [^{125}I]IBDG was achieved using a radioiododestannylation reaction followed by acetyl deprotection to afford [^{125}I]IBDG in >75% overall radiochemical yield and >99% chemical and radiochemical purity.

Prior to conducting *in vivo* studies we evaluated the specificity of [^{125}I]IBDG for cell uptake and retention in β-gal expressing cells using an *in vitro* cell uptake assay. The cellular trapping of [^{125}I]IBDG was evaluated at 3 substrate concentrations (0, 0.5 and 1.0 mM). In these studies, [^{125}I]IBDG displayed optimum cellular trapping of radioactivity (6.5 – 7-fold increase) in β-gal expressing D54 cells (*D54L*) as compared to control cells (*D54*) at the 0.5 mM substrate concentration. Importantly, we did not observe a significant difference in radioactivity uptake between the two cell types at either the 24 h or 48 h time interval in the absence of carrier (0 mM). This observation can be attributed to the fact that the IBDG substrate concentration was significantly lower relative to the enzymes' *Km* value which is reported to be in the 0.1 – 4 mM range.25

Encouraged by these initial findings, we administered [^{125}I]IBDG intravenously to CD1 mice having *D54L* and *D54* solid tumor xenografts and conducted serial SPECT/CT imaging studies. Since our *in vitro* cell uptake studies demonstrated optimal trapping of [^{125}I]IBDG at a 0.5 mM substrate concentration, radioligand doses were formulated at a similar IBDG concentration for the imaging studies. Visualization of either tumor was not possible throughout the 24 h imaging interval due to insufficient tumor uptake of radioactivity. Radioactivity clearance occurred mainly via the renal pathway as evidenced by high initial kidney uptake followed by excretion into bladder and the absence of radioactivity in liver. Negligible radioactivity levels were seen in most other organs including thyroid during the entire imaging sequence.

To confirm that the lack of tumor uptake of the radioligand was due to poor delivery to the tumor and not due to lack of β-gal enzyme recognition *in vivo*, SPECT imaging studies were repeated following direct intratumoral injection of [^{125}I]IBDG to *D54L* and *D54* tumors implanted in the same mouse on opposite flanks. Analysis of the SPECT image data revealed strikingly different kinetics of radioactivity clearance between the two tumor types. The fast clearance of radioactivity from the *D54* tumor site relative to the β-gal expressing *D54L* tumor enabled selective SPECT visualization of the *D54L* tumor at >4 h post-injection. Radioactivity clearance which occurred predominantly via renal excretion as seen

with the intravenous administration route resulted in high radioactivity levels in mouse bladder at early time intervals (2 h – 4 h), which, later declined to near background levels by 7 h post-injection. In addition, near background levels of radioactivity uptake were seen in most other organs including liver and thyroid, the latter indicative that [^{125}I]IBDG is relatively stable to *in vivo* metabolic deiodination.

Important requirements for a successful *in vivo* imaging radioligand include a high uptake in target tissues in conjunction with a rapid clearance from non-target tissues. Since β-gal is localized within the cytoplasm, the radioligand must be sufficiently hydrophobic to diffuse through the cell membrane to reach its intended target. Once inside the cell, the radiolabeled product resulting from enzymatic action should also demonstrate low diffusibility to ensure its cellular retention. Our intratumoral injection imaging data confirms that [^{125}I]IBDG (log P = 0.8) undergoes both facile cell permeation and selective intracellular trapping in *D54L* cells following enzymatic hydrolysis by β-gal. Furthermore, the rapid washout of radioactivity from the *D54* control cell site indicates that unprocessed radioligand is being efficiently cleared out of the cell and from the circulation into the renal compartment. In this regard, our biological results underscore the advantage of using radiolabeled enzyme substrates that afford trapping of the product of a catalytic reaction over inhibitors as radioligands for imaging enzyme expression since continuous enzyme processing of such substrates affords high signal amplification at the site of enzymatic processing.

The imaging data from the intratumoral injection studies suggested to us that limited delivery of the radioligand to tumors on systemic injection, which is likely due to high renal clearance, plays a key role in the observed lack of tumor uptake. To further understand the poor tumor-targeting behavior of [^{125}I]IBDG after systemic administration, blood metabolite analysis studies were conducted in tumor-bearing CD1 mice following intravenous injection of the radioligand. In these studies, the intact radioligand ([^{125}I]IBDG) accounted for less than 40% of the total radioactivity present in mouse blood at 5 min post-injection. The remaining radioactivity comprised of two polar metabolites, which we confirmed were not [^{125}I]iodide by radio-HPLC analysis. Importantly, the total blood radioactivity in a mouse at 5 min post-injection was only 13 – 15 μCi following a 600 μCi injection of [^{125}I]IBDG. Since only renal and bladder radioactivity were apparent in the early SPECT images, this data further confirms that the majority of the systemically administered [^{125}I]IBDG is being rapidly excreted in urine either as the intact radioligand or as a metabolite.

In summary, we synthesized and evaluated a radioiodinated β-gal substrate ([^{125}I]IBDG) as a radioligand for *in vivo* SPECT imaging of tumor β-galactosidase enzyme expression. Although [^{125}I]IBDG showed high differential uptake (6.5 – 7-fold) in β-galactosidase expressing tumor cells over control cells in *in vitro* studies it demonstrated insufficient uptake in β-gal expressing tumors for SPECT imaging upon systemic injection. However, SPECT imaging of CD1 mice following direct intratumoral injection of [^{125}I]IBDG to β-gal expressing *D54L* tumors and control *D54* tumors co-implanted in the same mouse demonstrated selective retention of radioactivity at the *D54L* tumor at 2 h through 7 h post-injection resulting in clear visualization of this tumor. Analysis of the imaging and blood metabolite profile data suggest that the poor tumor localization of [^{125}I]IBDG is likely a result of high and rapid renal excretion. Thus, despite useful biological characteristics such as good cell permeability, substrate specificity and fast clearance from non-target tissues, our studies indicate that [^{125}I]IBDG is unsuitable for the *in vivo* imaging of β-gal expression. We conclude that further structural modification of IBDG to retard its renal clearance and improve cell uptake or the evaluation of alternative β-gal substrates with improved pharmacokinetic properties is warranted to improve the β-gal expression imaging capability of this class of radioligands. These studies are currently underway in our laboratory.

Abbreviations

β-gal	beta-galactosidase
IBDG	5-Iodoindol-3-yl-β-D-galactopyranoside
SPECT	single photon emission computed tomography
PET	positron emission tomography

Acknowledgments

The authors acknowledge support for this work from the following National Institutes of Health Grants: PO1-CA85878, P50-CA093990 and R24-CA083099. We thank Dr. Mahaveer S. Bhojani for helpful discussions and technical assistance with the Figures.

REFERENCES

1. Schenborn E, Groskreutz D. Reporter gene vectors and assays. Mol Biotechnol. 1999; 13:29–44. [PubMed: 10934520]
2. Kamiya M, Kobayashi H, Hama Y, Koyama Y, Bernardo M, Nagano T, Choyke PL, Urano Y. An enzymatically activated fluorescence probe for targeted tumor imaging. J Am Chem Soc. 2007; 129:3918–3929. [PubMed: 17352471]
3. Chilvers KF, Perry JD, James AL, Reed RH. Synthesis and evaluation of novel fluorogenic substrates for the detection of bacterial beta-galactosidase. J Appl Microbiol. 2001; 91:1118–1130. [PubMed: 11851821]
4. Pocsi I, Taylor SA, Richardson AC, Smith BV, Price RG. Comparison of several new chromogenic galactosides as substrates for various beta-D-galactosidases. Biochim Biophys Acta. 1993; 1163:54–60. [PubMed: 8476929]
5. Blasberg R. PET imaging of gene expression. Eur J Cancer. 2002; 38:2137–2146. [PubMed: 12387839]
6. Haberkorn U, Mier W, Eisenhut M. Scintigraphic imaging of gene expression and gene transfer. Current medicinal chemistry. 2005; 12:779–794. [PubMed: 15853711]
7. Herschman HR. PET reporter genes for noninvasive imaging of gene therapy, cell tracking and transgenic analysis. Critical reviews in oncology/hematology. 2004; 51:191–204. [PubMed: 15331078]
8. Ho NH, Weissleder R, Tung CH. A self-immolative reporter for beta-galactosidase sensing. Chembiochem. 2007; 8:560–566. [PubMed: 17300128]
9. Josserand V, Texier-Nogues I, Huber P, Favrot MC, Coll JL. Non-invasive in vivo optical imaging of the lacZ and luc gene expression in mice. Gene Ther. 2007; 14:1587–1593. [PubMed: 17882264]
10. Tung CH, Zeng Q, Shah K, Kim DE, Schellingerhout D, Weissleder R. In vivo imaging of beta-galactosidase activity using far red fluorescent switch. Cancer Res. 2004; 64:1579–1583. [PubMed: 14996712]
11. Wehrman TS, von Degenfeld G, Krutzik PO, Nolan GP, Blau HM. Luminescent imaging of beta-galactosidase activity in living subjects using sequential reporter-enzyme luminescence. Nat Methods. 2006; 3:295–301. [PubMed: 16554835]
12. Louie AY, Huber MM, Ahrens ET, Rothbacher U, Moats R, Jacobs RE, Fraser SE, Meade TJ. In vivo visualization of gene expression using magnetic resonance imaging. Nat Biotechnol. 2000; 18:321–325. [PubMed: 10700150]
13. Choi JH, Choe YS, Lee KH, Choi Y, Kim SE, Kim BT. Synthesis of radioiodine-labeled 2-phenylethyl 1-thio-beta-D-galactopyranoside for imaging of LacZ gene expression. Carbohydr Res. 2003; 338:29–34. [PubMed: 12504378]
14. Lee KH, Byun SS, Choi JH, Paik JY, Choe YS, Kim BT. Targeting of lacZ reporter gene expression with radioiodine-labelled phenylethyl-beta- d-thiogalactopyranoside. Eur J Nucl Med Mol Imaging. 2004; 31:433–438. [PubMed: 14745516]

15. Kiernan JA. Indigogenic substrates for detection and localization of enzymes. Biotech Histochem. 2007; 82:73–103. [PubMed: 17577701]
16. Horwitz JP, Chua J, Curby RJ, Tomson AJ, Darooge MA, Fisher BE, Mauricio J, Klundt I. Substrates for Cytochemical Demonstration of Enzyme Activity. I. Some Substituted 3-Indolyl-Beta-D-Glycopyranosides. J Med Chem. 1964; 7:574–575. [PubMed: 14221156]
17. Van Dort ME, Jung YW, Gildersleeve DL, Hagen CA, Kuhl DE, Wieland DM. Synthesis of the 123I-and 125I-labeled cholinergic nerve marker (−)-5-iodobenzovesamicol. Nuclear medicine and biology. 1993; 20:929–937. [PubMed: 8298572]
18. Rothwell JA, Day AJ, Morgan MR. Experimental determination of octanol-water partition coefficients of quercetin and related flavonoids. J Agric Food Chem. 2005; 53:4355–4360. [PubMed: 15913295]
19. Dess DK HP, Weinberg DV, Kaufman RJ, Sidhu RS. Phase-Transfer Catalyzed Synthesis of Acetylated Aryl b-D-Glucopyranosides and Aryl b-D-Galactopyranosides. Synthesis. 1981:883–885.
20. Kleine HPW DV, Kaufman RJ, Sidhu RS. Phase-transfer-catalyzed synthesis of 2,3,4,6-tetra-O-acetyl-b-D-galactopyranosides. Carbohydrate Research. 1985; 142:333–337.
21. Hatch N, Sarid J. Glial fibrillary acidic protein transcriptional regulation is independent of a TFIID-binding downstream initiator sequence. Journal of neurochemistry. 1994; 63:2003–2009. [PubMed: 7964717]
22. Cohen JC, Larson JE, Killeen E, Love D, Takemaru K. CFTR and Wnt/beta-catenin signaling in lung development. BMC developmental biology. 2008; 8:70. [PubMed: 18601749]
23. Ding Z, Maubach G, Masamune A, Zhuo L. Glial fibrillary acidic protein promoter targets pancreatic stellate cells. Dig Liver Dis. 2008
24. Jeong JH, Jin JS, Kim HN, Kang SM, Liu JC, Lengner CJ, Otto F, Mundlos S, Stein JL, van Wijnen AJ, Lian JB, Stein GS, Choi JY. Expression of Runx2 transcription factor in non-skeletal tissues, sperm and brain. Journal of cellular physiology. 2008
25. Weber K, Sund H, Wallenfels K. [on the Nature of the Binding between Subunits in the Molecule of Beta-Galactosidase from E. Coli.]. Biochemische Zeitschrift. 1964; 339:498–500. [PubMed: 14243756]

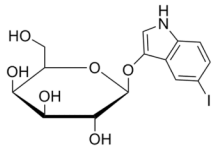

5-Iodoindol-3-yl-β-D-galactopyranoside (IBDG)

Figure 1.
Structure of IBDG

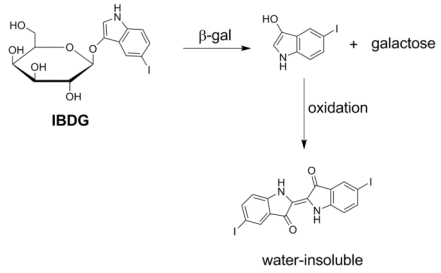

Figure 2.
Enzymatic hydrolysis of IBDG by β-Galactosidase

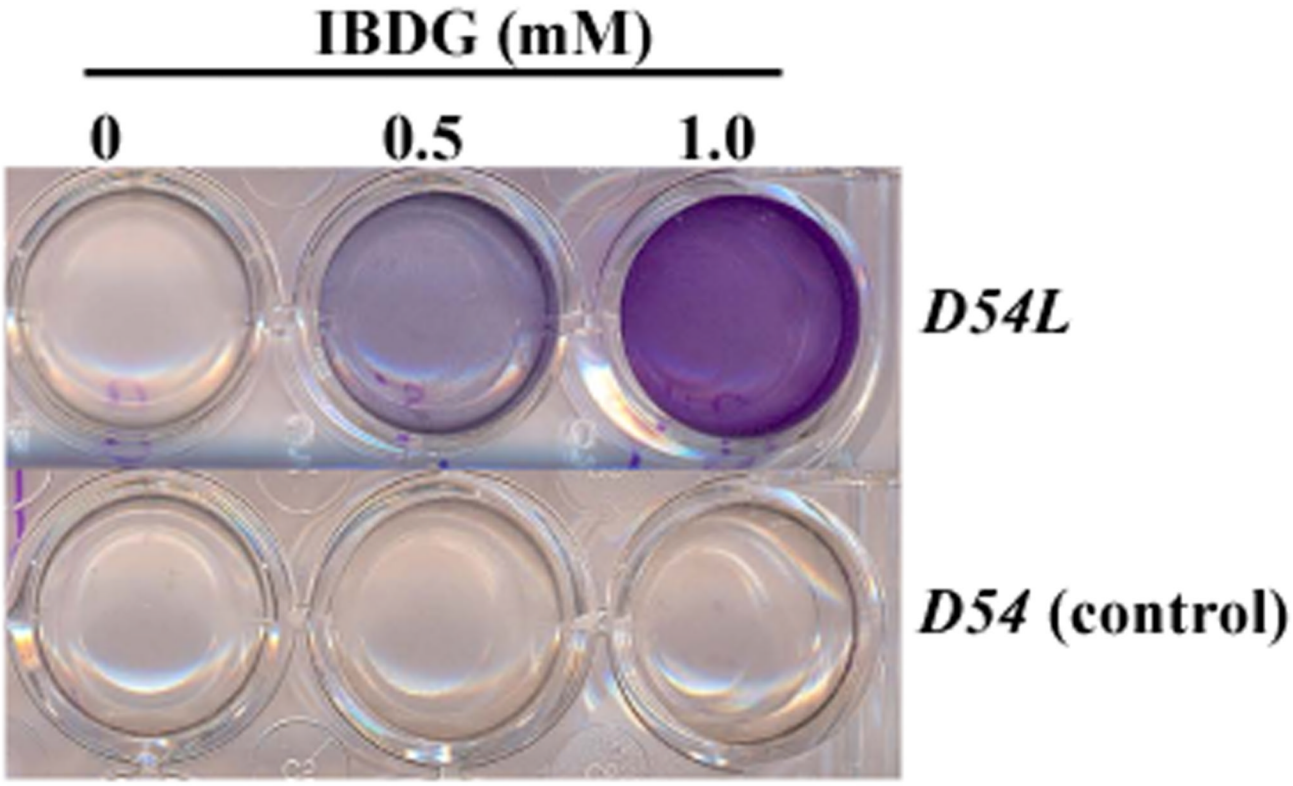

Figure 3.

β-Galactosidase dependent staining of D54 cells in the presence of IBDG. Control D54 human glioma cells (*D54*) or their β-galactosidase-expressing counterpart (*D54L*) were cultured in 6-well dishes and treated with 0, 0.5 or 1.0 mM IBDG for 24 h. Experiments were conducted in triplicate. Hydrolysis of IBDG is visualized by virtue of the formation of a violet precipitate in *D54L* cells but not in *D54* cells.

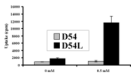

Figure 4.

Comparison of cellular uptake of [^{125}I]IBDG in *D54* and *D54L* cells at 24 h incubation. Control D54 human glioma cells (*D54*) or their β-galactosidase-expressing counterpart (*D54L*) were incubated for 24 h in 6-well dishes with various concentrations of cold IBDG (0, 0.5 mM) spiked with [^{125}I]IBDG (0.1 μCi per well). Data points represent the mean ± SD of triplicate determinations. Cellular uptake of radioactivity is reported in units of counts per min (cpm).

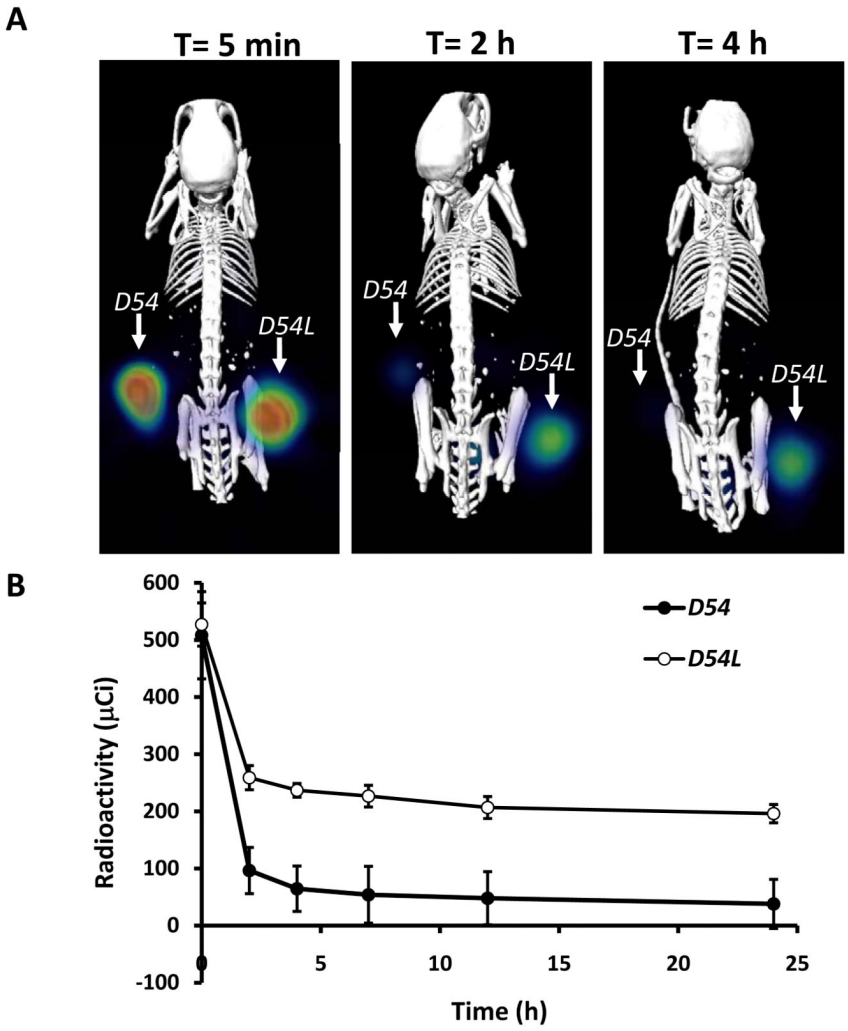

Figure 5.

(A). Co-registered SPECT/CT images in a CD1 mouse after [^{125}I]IBDG administration to control *D54* tumors (left flank) and β-gal-expressing *D54L* tumors (right flank). **(B).** Time-radioactivity curves of administered [^{125}I]IBDG in mouse *D54* and *D54L* tumors.

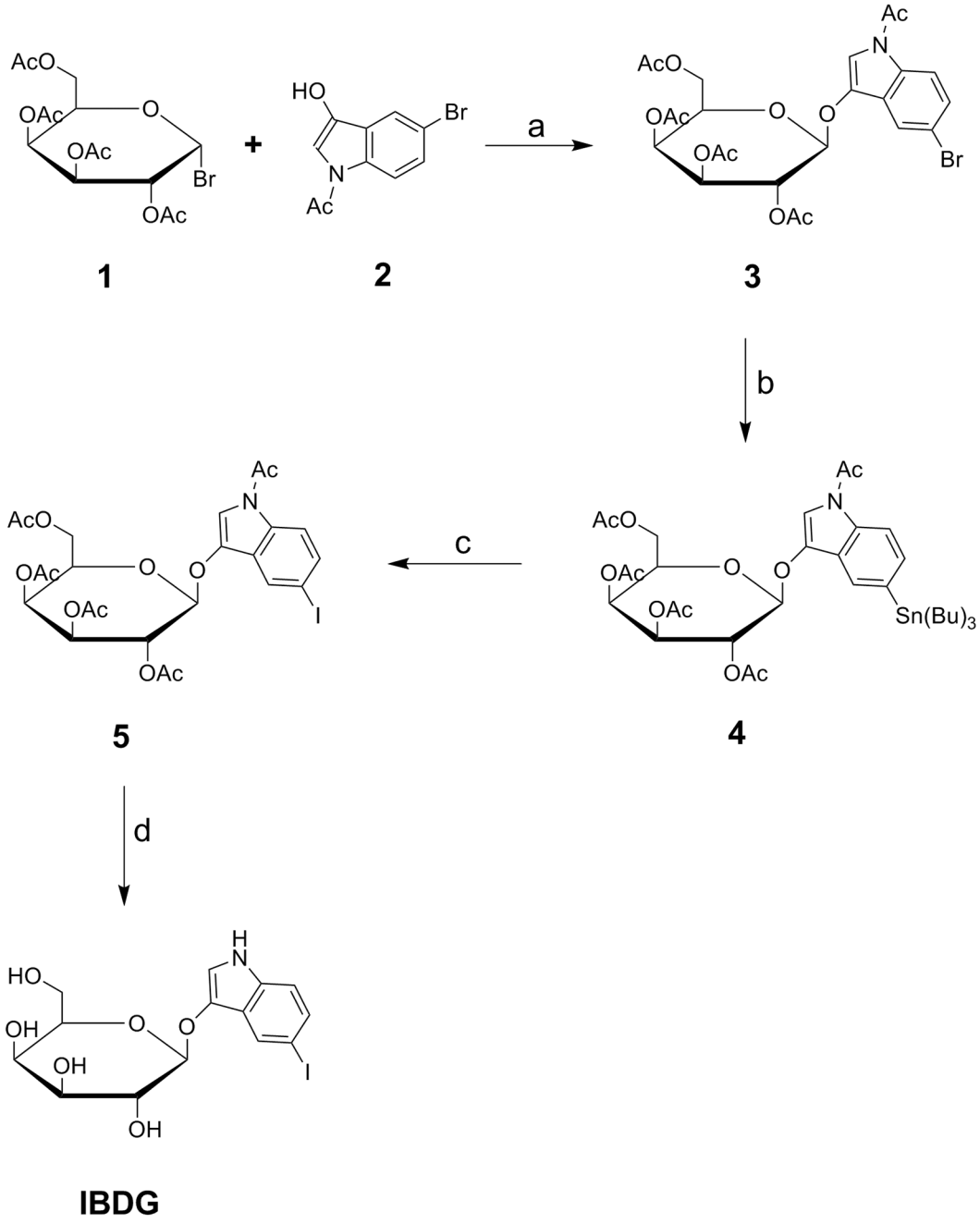

SCHEME 1a.

[a] Reagents and conditions: (a) 1 N NaOH, acetone, 5 °C; (b) $Pd(PPh_3)_4$, Sn_2Bu_6, toluene, reflux; (c) I_2, $ChCl_3$, rt; (d) NaOMe, MeOH, 5 °C.

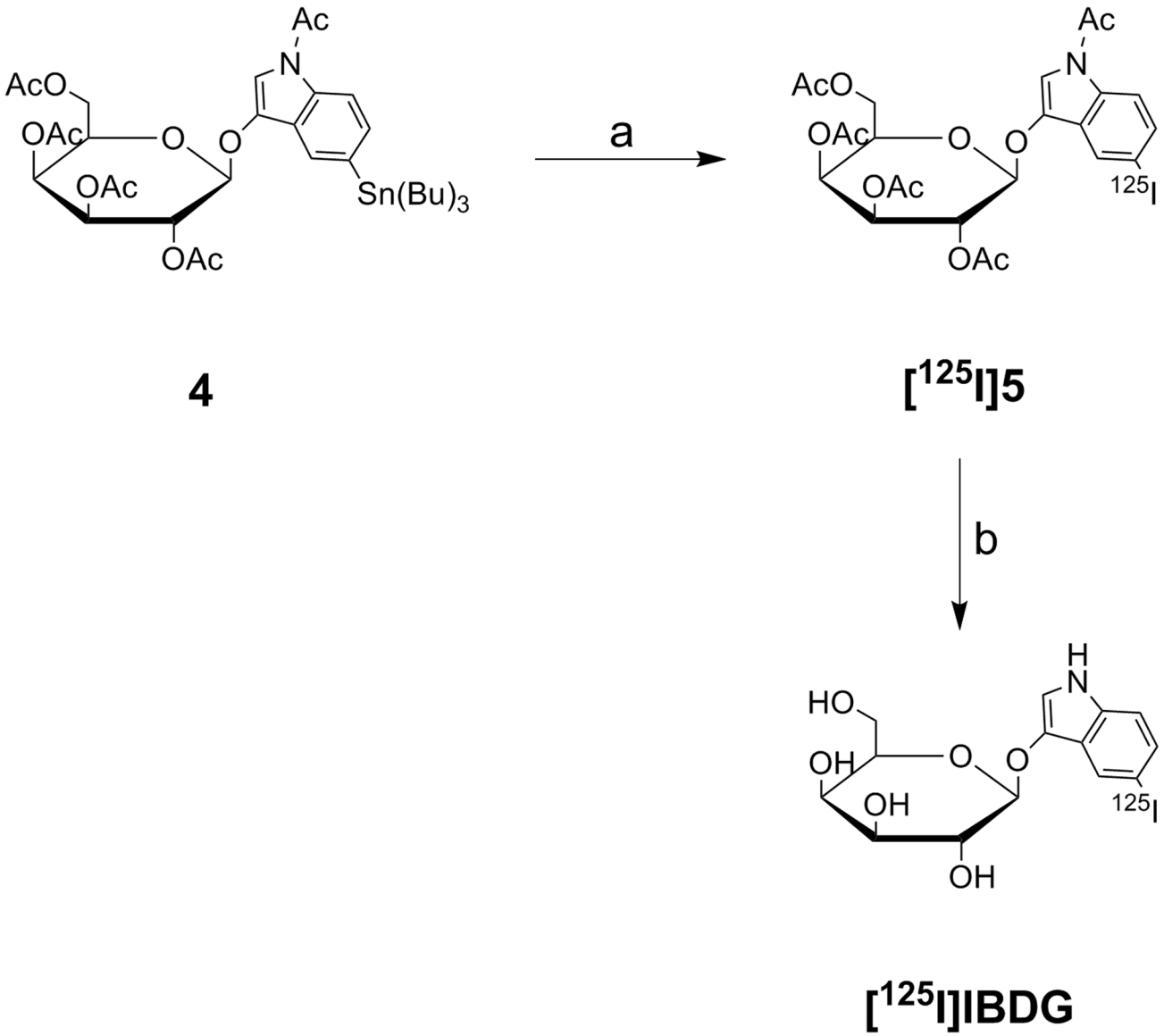

SCHEME 2a.

[a] Reagents and conditions: (a) $Na^{125}I$, H_2O_2, 0.1 N ethanolic HCl; (b) NaOMe, MeOH, 5 °C.